Omidi, Milad; St-Pierre, Luc

The fracture toughness of demi-regular lattices

Published in:
Scripta Materialia

DOI:
10.1016/j.scriptamat.2023.115686

Published: 01/12/2023

Document Version
Publisher's PDF, also known as Version of record

Scripta Materialia 237 (2023) 115686

Contents lists available at ScienceDirect

Scripta Materialia

journal homepage: www.journals.elsevier.com/scripta-materialia

The fracture toughness of demi-regular lattices

Milad Omidi, Luc St-Pierre *

Department of Mechanical Engineering, Aalto University, Espoo 02150, Finland

ARTICLE INFO

Keywords:
Cellular materials
Fracture
Toughness
Finite element analysis
Demi-regular tessellations

ABSTRACT

The properties of lattices are strongly influenced by their nodal connectivity; yet, previous studies have focused mainly on topologies with a single vertex configuration. This work investigates the potential of demi-regular lattices, with two vertex configurations, to outperform existing topologies, such as triangular and kagome lattices. We used finite element simulations to predict the fracture toughness of three elastic-brittle demi-regular lattices under modes I, II, and mixed-mode loading. The fracture toughness of two demi-regular lattices scales linearly with relative density $\bar{\rho}$, and outperforms a triangular lattice by 15% under mode I and 30% under mode II. The third demi-regular lattice has a fracture toughness K_{Ic} that scales with $\sqrt{\bar{\rho}}$ and matches the remarkable toughness of a kagome lattice. Finally, a kinematic matrix analysis revealed that topologies with $K_{Ic} \propto \sqrt{\bar{\rho}}$ have periodic mechanisms and this may be a key feature explaining their high fracture toughness.

Lattice materials are well known for their ability to be stiff and strong at low densities [1–6], but their architecture can also be tailored to achieve a high fracture toughness [7–10]. While the stiffness and strength of lattices are limited by bounds, and architectures approaching those limits have been identified [11–13], their fracture toughness is not theoretically bounded. Relatively few topologies have been investigated so far in the quest to maximise fracture toughness; therefore, the aim of this study is to discover tougher lattice materials by exploring novel architectures.

The influence of topology on fracture toughness has been documented predominantly for planar lattices. Analytical [14–18], numerical [19–25] and experimental [26–29] studies have shown that the fracture toughness of an elastic-brittle lattice can be expressed as:

$$\frac{K_{Ic}}{\sigma_{ts}\sqrt{\ell}} = D_I \bar{\rho}^d \qquad \text{and} \qquad \frac{K_{IIc}}{\sigma_{ts}\sqrt{\ell}} = D_{II} \bar{\rho}^d, \tag{1}$$

where K_{Ic} and K_{IIc} are the fracture toughness under mode I and II, respectively; $\bar{\rho}$ is the relative density of the lattice; ℓ is the length of the cell walls; σ_{ts} is the tensile strength of the parent material; and the constants D_I, D_{II}, and d are given in Table 1 for planar transversely isotropic lattices, which are shown in Fig. 1. Orthotropic topologies, such as the square or snub-square lattices, have also been investigated but they do not outperform the toughest isotropic lattices [20,21,27,30,31].

The exponent d has a strong effect on the fracture toughness: a lower d leads to a higher fracture toughness at low relative densities $\bar{\rho}$, see (1). The exponent d is insensitive to the choice of parent material [32], and strongly influenced by the lattice's nodal connectivity (the number of bars meeting at each joint). With three bars per joint, the hexagonal lattice (Fig. 1a) deforms by bending, and this leads to a particularly low fracture toughness with $d = 2$ [14,15,33,34]. In contrast, the triangular lattice (Fig. 1b), with six bars per joint, and the snub-trihexagonal architecture (Fig. 1c), with five bars per joint, are stretching-dominated meaning that their members carry predominantly axial stresses. This mode of deformation leads to a fracture toughness that scales linearly with relative density, with an exponent $d = 1$ [19,31,35]. Finally, the kagome lattice (Fig. 1d), with four bars per joint, has an unusual behaviour. It is stretching-dominated, as stiff and strong as a triangular lattice [2], but its fracture toughness scales with the square-root of relative density ($d = 0.5$), making it remarkably tough at low values of $\bar{\rho}$. This exceptional toughness is due to a crack tip blunting phenomenon caused by localised bending deformation [19,32]. The kagome lattice is the only known topology with $d = 0.5$, and it is unclear if other architectures could match or exceed its toughness.

All architectures investigated so far share a similar characteristic: they have a unique vertex configuration (meaning that each vertex inside a given lattice has the same sequence of polygons, see Fig. 1a-d). In geometry, these are referred to as 1-uniform tilings and include *regular* tessellations (made from a single regular polygon *e.g.* hexagonal and triangular lattices) and *semi-regular* lattices (assembled from two or more regular polygons *e.g.* snub-trihexagonal and kagome lattices) [36]. Considering the importance of nodal connectivity on fracture toughness,

* Corresponding author.
E-mail address: luc.st-pierre@aalto.fi (L. St-Pierre).

https://doi.org/10.1016/j.scriptamat.2023.115686
Received 8 May 2023; Received in revised form 10 July 2023; Accepted 26 July 2023
Available online 3 August 2023

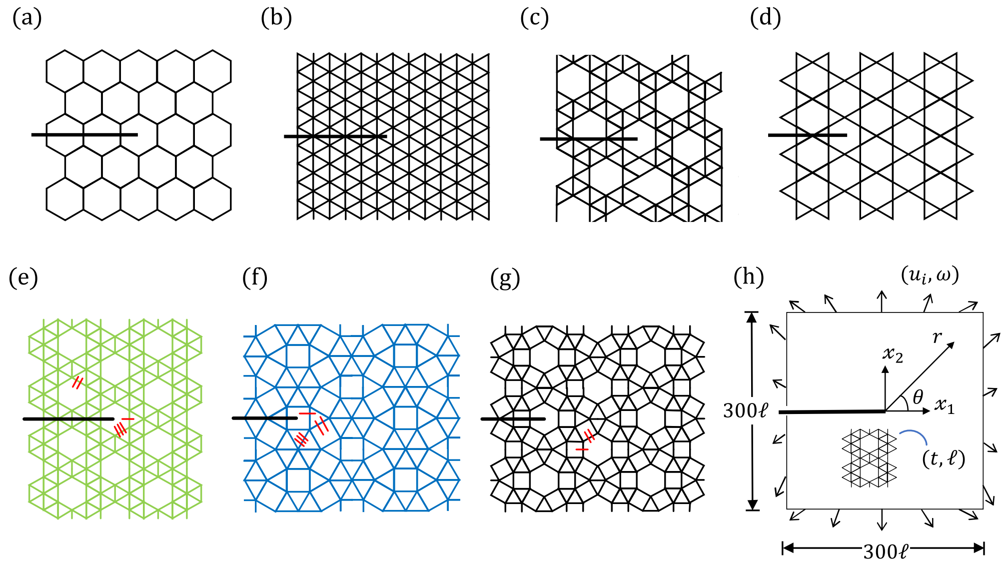

Fig. 1. The seven planar lattices listed in Table 1. The (a) hexagonal, (b) triangular, (c) snub-trihexagonal, and (d) kagome lattices were investigated previously [19,31], whereas this paper focuses on demi-regular lattices (e) A, (f) B, and (g) C. The thick black line indicates the position of the initial crack. Fracture sites under mixed-mode loading are shown with |, ||, and ||| symbols for demi-regular lattices. (h) Domain and coordinate system used in our finite element predictions.

Table 1
Constants D_I, D_{II}, and d in (1) for planar transversely isotropic lattice materials. These topologies are shown in Fig. 1.

Topology	D_I	D_{II}	d	Reference
Hexagonal	0.800	0.370	2	[19]
Triangular	0.500	0.380	1	[19]
Snub-trihexagonal	0.460	—	1	[31]
Kagome	0.212	0.133	0.5	[19]
A	0.570	0.510	1	This study
B	0.580	0.490	1	This study
C	0.210	0.150	0.5	This study

and to broaden the search for tougher architectures, we turn our attention to lattices with two different vertex configurations. These are called 2-uniform or *demi-regular* lattices [37]. Three examples are shown in Fig. 1e-g: demi-regular lattices A and B have joints with five and others with six bars, whereas the vertices of tessellation C have either four or five struts. These three demi-regular lattices were recently shown to be stretching-dominated and transversely isotropic, with an elastic modulus that is comparable but slightly lower than that of kagome and triangular lattices [38]. The aim of this study is to characterise the fracture behaviour of these three demi-regular lattices and evaluate if they are tougher than other stretching-dominated architectures, such as kagome and triangular lattices.

The fracture toughness of each demi-regular lattice was predicted using Finite Element (FE) simulations; more specifically, with the static implicit solver of the commercial software Abaqus. Our modelling approach relied on the boundary layer method, as used in previous studies [19,21,31,34,35], to ensure that our results can be compared directly those in Table 1.

For each demi-regular lattice, a large square domain was created with a side length of 300ℓ, where ℓ is the length of a cell wall (see Fig. 1h). The domain included a semi-infinite crack along the negative x_1 axis and a detailed view showing the position of the crack tip for each topology is given in Fig. 1e-g. Numerical experimentation showed that moving the crack tip to another cell or changing the crack orientation have a negligible effect on the fracture toughness. In Supplementary material, we show that (i) our domain is sufficiently large to ensure that predictions are size-independent, and (ii) the crack orientation considered in Fig. 1e-g is the one associated with the lowest mode I fracture toughness.

The cell walls were meshed using Timoshenko beam elements (B21 in Abaqus notation). A fine mesh size of $\ell/30$ was used within a $60\ell \times 60\ell$ area centred at the crack tip, whereas a coarser mesh size of $\ell/10$ was employed elsewhere. Further mesh refinements had an imperceptible effect on the results. The relative density $\bar{\rho}$ was varied from 0.01 to 0.2 by changing the strut thickness t while keeping the strut length ℓ fixed. The relationship between $\bar{\rho}$ and t/ℓ is given in Supplementary material for each demi-regular lattice.

Each node on the domain's perimeter was subjected to a displacement corresponding to the asymptotic crack tip solution from linear elastic fracture mechanics. The displacement field included two translations, u_1 and u_2, and an in-plane rotation ω, see Fig. 1h. Expressions for u_1, u_2, and ω are lengthy and provided in Supplementary material. They are functions of the nodal coordinates (r, θ); the elastic properties of the lattice given in [38]; and the applied stress intensify factors K_I and K_{II} for modes I and II, respectively. Our approach is identical to that used by Fleck and Qiu [19] to predict the fracture toughness of other planar transversely isotropic lattices.

The cell walls were modelled as an elastic-brittle material, characterised by a Young's modulus E_s and Poisson ratio ν_s, up to a tensile fracture strength σ_{ts}. In our simulations, the fracture toughness K_{Ic} (or K_{IIc}) corresponded to the value of K_I (or K_{II}) when the maximum tensile stress in any element of the lattice reached the strength of the parent material σ_{ts}.

The fracture toughness of each demi-regular lattice is plotted as a function of relative density in Fig. 2a for mode I and Fig. 2b for mode II. In each plot, the fracture toughness is normalised by $\sigma_{ts}\sqrt{\ell}$ based on the scaling law given in (1). Deformed meshes for each topology with $\bar{\rho} = 0.05$ are given in Fig. 3 for both modes I and II.

The fracture toughness of demi-regular lattices A and B scales linearly with relative density, see Fig. 2, corresponding to an exponent $d = 1$ in (1). In contrast, the fracture toughness of tessellation C scales with $\sqrt{\bar{\rho}}$, giving $d = 0.5$. With a lower value of d, lattice C is significantly tougher than topologies A and B at low relative densities. This holds true for both K_{Ic} and K_{IIc} as the exponent d is the same for both modes I and II. The lower value of d for topology C is due to crack tip blunting, which does not occur in tessellations A and B, see Fig. 3.

The results in Fig. 2 were used to evaluate the constants D_I and D_{II} in (1) and their values are given in Table 1. For each demi-regular lattice, $D_I > D_{II}$ meaning that fracture toughness is higher for mode I than mode II. The differences are, however, sensitive to topology; the ratios

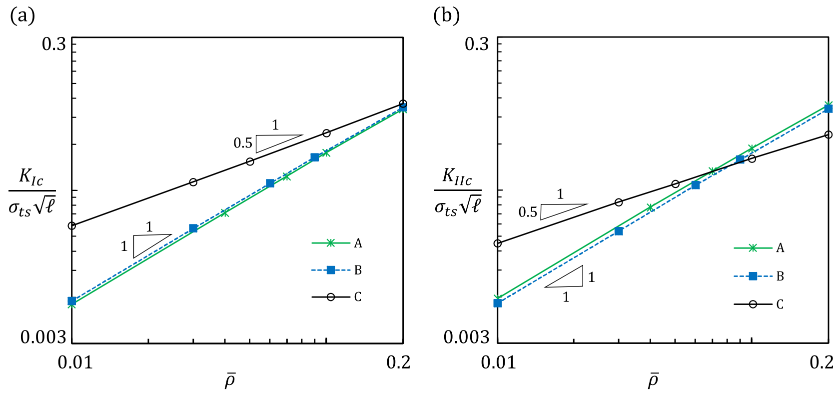

Fig. 2. Fracture toughness under (a) mode I and (b) mode II, as a function of relative density $\bar{\rho}$. Results are given for demi-regular lattices A, B, and C.

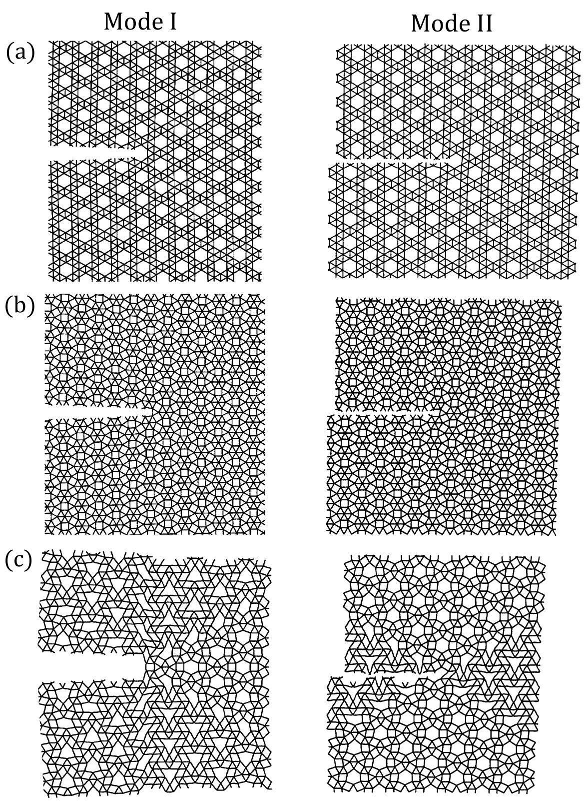

Fig. 3. Deformed meshes for demi-regular lattices (a) A, (b) B, and (c) C. Results are shown for mode I (left) and mode II (right) loading. All lattices have a relative density $\bar{\rho} = 0.05$.

K_{Ic}/K_{IIc} are 1.12, 1.18 and 1.40 for tessellations A, B, and C, respectively. Demi-regular lattices A and B have a similar fracture toughness, which is roughly 15% higher than a triangular lattice under mode I, and approximately 30% tougher in mode II, see Table 1. Otherwise, tessellation C and the kagome lattice have practically the same K_{Ic} and K_{IIc}.

The fracture envelope under mixed-mode loading is plotted in Fig. 4a for demi-regular lattices A and B, and in Fig. 4b for tessellation C. Based on the results in Fig. 2, the stress intensity factors K_I and K_{II} are normalised here by $\sigma_{ts}\bar{\rho}\sqrt{\ell}$ for lattices A and B, and by $\sigma_{ts}\sqrt{\bar{\rho}\ell}$ for tessellation C. This normalisation ensures that each fracture envelope is independent of relative density $\bar{\rho}$. Each envelope is formed by two or three straight lines, where each segment corresponds to a different fracture location. The segments are labelled |, ||, and ||| in Fig. 4, and the corresponding fracture locations are shown in Fig. 1. For comparison, results for the triangular and kagome lattices are included in Fig. 4a and b, respectively. Their envelopes were obtained using the same modelling approach detailed above and their crack orientations are given in Fig. 1.

Table 2
Elastic modulus E, Poisson's ratio ν, tensile strength σ_c, fracture toughness K_{Ic}, transition flaw size a_t, and toughness G_c of triangular, kagome, and demi-regular lattices. All properties are given in a non-dimensional form. Note that E, ν, and σ_c were collected from [2,38], and σ_c is the tensile strength in x_2, see Fig. 1.

Topology	E/E_s	ν	σ_c/σ_{ts}	$K_{Ic}/(\sigma_{ts}\sqrt{\ell})$	a_c/ℓ	$G_{Ic}E_s/(\sigma_{ts}\ell)$
Triangular	$0.333\bar{\rho}$	0.333	$0.333\bar{\rho}$	$0.500\bar{\rho}$	0.717	$0.666\bar{\rho}$
A	$0.292\bar{\rho}$	0.364	$0.268\bar{\rho}$	$0.570\bar{\rho}$	1.440	$0.965\bar{\rho}$
B	$0.318\bar{\rho}$	0.362	$0.304\bar{\rho}$	$0.580\bar{\rho}$	1.158	$0.919\bar{\rho}$
Kagome	$0.333\bar{\rho}$	0.333	$0.333\bar{\rho}$	$0.212\sqrt{\bar{\rho}}$	$0.129/\bar{\rho}$	0.120
C	$0.260\bar{\rho}$	0.455	$0.214\bar{\rho}$	$0.210\sqrt{\bar{\rho}}$	$0.306/\bar{\rho}$	0.135

The fracture envelopes of lattices A and B are close to a quarter circle, whereas that of tessellation C has two straight sides, see Fig. 4. Demi-regular lattice C and the kagome topology have very similar fracture envelopes, but tessellations A and B both outperform the triangular lattice under mixed-mode loading. Quantitatively, the area contained within the fracture envelope of tessellation A is 43% larger than that of a triangular lattice.

For topologies A and B, fracture takes place in the vertical bar in front of the crack tip when $K_I \gg K_{II}$ and moves off the crack plane when K_{II} increases, see Fig. 1e,f. In contrast, the fracture sites in tessellation C are always off the crack plane and located a few cells away from the crack tip. These results are in-line with the observations of Fleck and Qiu [19]: they found that fracture sites in a triangular lattice are within a distance ℓ of the crack tip, whereas those in a kagome lattice are located at $\approx 3\ell$ from the crack tip.

Fracture toughness is not the only property to consider in material selection; the elastic modulus E and tensile fracture strength σ_c also influence design choices depending on the application. These properties are compared in Table 2 for triangular, kagome, and demi-regular lattices. Demi-regular architectures are 5-22% more compliant and 8-35% weaker than triangular and kagome lattices. Demi-regular lattices, however, have a fracture toughness equal or superior to that of other topologies.

In load-limited design, the maximum stress that a lattice panel with a central crack can carry will switch from σ_c to a lower value $\sigma = K_{Ic}/\sqrt{\pi a}$ as the crack length a increases. This change will occur at a transition flaw size [1,19]:

$$a_t = \frac{1}{\pi}\left(\frac{K_{Ic}}{\sigma_c}\right)^2, \tag{2}$$

which is also listed in Table 2. Clearly, demi-regular lattices are more damage tolerant than other topologies. For tessellations A and B, the

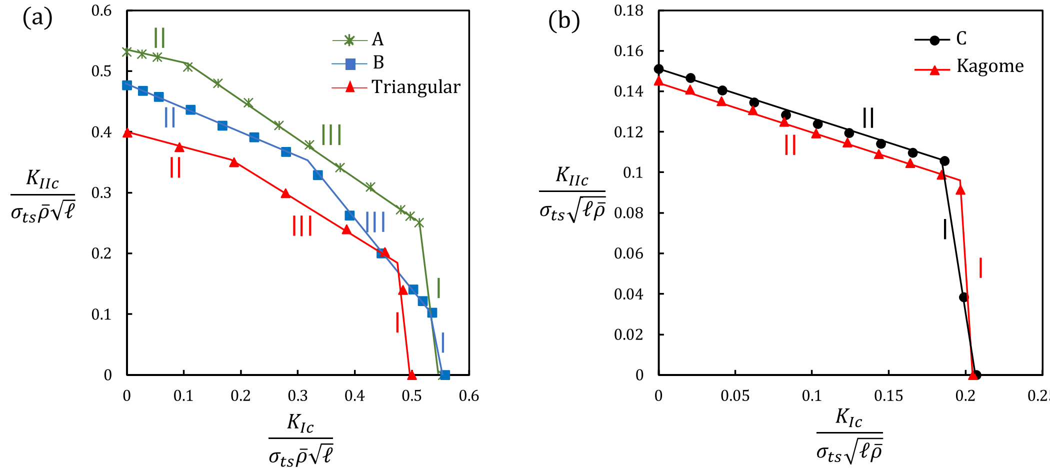

Fig. 4. Mixed-mode fracture envelopes: (a) demi-regular lattices A and B are compared to a triangular tessellation and (b) demi-regular lattice C is compared to a kagome tessellation. The segments labelled |, ||, and ||| correspond to different fracture sites, which are shown in Fig. 1.

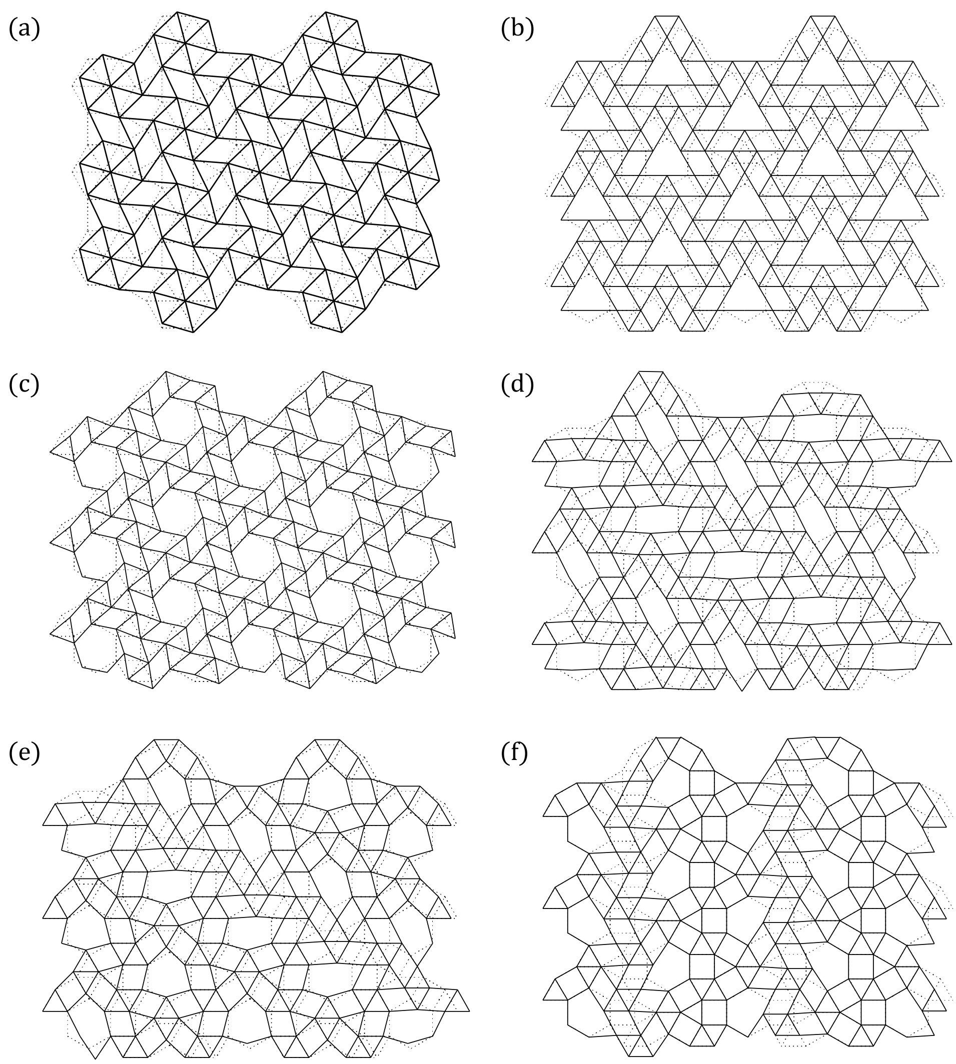

Fig. 5. (a) The single 1-periodic mechanism of demi-regular lattice B. (b,c) The two 1-periodic mechanisms of demi-regular lattice C. Tessellation C also has N-periodic mechanisms: examples of (d) 2-periodic, (e) 3-periodic, and (f) 4-periodic mechanisms along the 30° direction.

transition flaw size is independent of $\bar{\rho}$ and is 1.6-2 times larger than that of a triangular lattice. In contrast, $a_t \propto 1/\bar{\rho}$ for tessellation C and its transition flaw size is 2.4 times higher than that of a kagome lattice.

In some applications, it is necessary to maximise the energy stored before fracture, and this requires a material with a high toughness $G_{Ic} = (1-\nu^2)K_{Ic}^2/E$ [39]. This property is also included in Table 2.

Demi-regular lattices A and B have a toughness $G_{Ic} \propto \bar{\rho}$, which is about 40% higher than that of a triangular lattice. Otherwise, tessellation C and the kagome lattice have a similar toughness, which is, remarkably, independent of relative density.

Lattices with $d = 1/2$, such as kagome and tessellation C, are highly desirable; yet, the characteristics that lead to this behaviour are unknown. Here, we hypothesise that a stretching-dominated lattice should have periodic mechanisms to have $d = 1/2$. This is based on the fact that the kagome lattice has many periodic mechanisms [40–42], whereas a triangular lattice has none.

The mechanisms of each demi-regular lattice were analysed to test the validity of our hypothesis. We used the Bloch wave approach [41] and all details are provided in Supplementary material. Below, we will describe a mechanism as N-periodic if its deformation has a wavelength of N unit cells [42].

Our analysis showed that demi-regular lattice A has no mechanisms, see Supplementary material. Otherwise, tessellation B has a single 1-periodic mechanism, see Fig. 5a. In contrast, demi-regular lattice C has two 1-periodic mechanisms (Fig. 5b,c) and many N-periodic mechanisms, with some examples given in Fig. 5d-f. Note the similarity between the mechanism in Fig. 5b and the deformed meshes in Fig. 3c. The kagome lattice and tessellation C are the only stretching-dominated topologies known to the authors to have such a large number of N-periodic mechanisms. While the evidence is limited, we believe that this may be a key feature leading to crack tip blunting and explaining the high fracture toughness of these two topologies.

In summary, we showed that three previously unexplored demi-regular lattices have a remarkably high fracture toughness. Demi-regular lattices A and B have a fracture toughness that scales linearly with relative density and are tougher than a triangular lattice under mode I, mode II, and mixed-mode loading conditions. Previously, the kagome lattice was the only known topology with a fracture toughness that scales with the square-root of relative density. We discovered that demi-regular lattice C exhibits the same scaling, and has a fracture toughness equal to that of a kagome lattice. Further analysis showed that the kagome lattice and tessellation C both have many N-periodic mechanisms, and additional work is needed to confirm/rebut that this is the main feature explaining their high fracture toughness.

Declaration of competing interest

The authors declare that they have no known competing financial interests or personal relationships that could have appeared to influence the work reported in this paper.

Acknowledgements

This work was supported by the Academy of Finland (grant 322007).

Appendix A. Supplementary material

Supplementary material related to this article can be found online at https://doi.org/10.1016/j.scriptamat.2023.115686.

References

[1] N.A. Fleck, V.S. Deshpande, M.F. Ashby, Micro-architectured materials: past, present and future, Proc. R. Soc. A, Math. Phys. Eng. Sci. 466 (2010) 2495–2516.
[2] A.-J. Wang, D.L. McDowell, In-plane stiffness and yield strength of periodic metal honeycombs, J. Eng. Mater. Technol. 126 (2004) 137–156.
[3] M. Omidi, L. St-Pierre, Mechanical properties of semi-regular lattices, Mater. Des. 213 (2022) 110324.
[4] S. Torquato, L.V. Gibiansky, M.J. Silva, L.J. Gibson, Effective mechanical and transport properties of cellular solids, Int. J. Mech. Sci. 40 (1998) 71–82.
[5] F. Côté, V.S. Deshpande, N.A. Fleck, A.G. Evans, The compressive and shear responses of corrugated and diamond lattice materials, Int. J. Solids Struct. 43 (2006) 6220–6242.
[6] A. Markou, L. St-Pierre, A novel parameter to tailor the properties of prismatic lattice materials, Int. J. Mech. Sci. 219 (2022) 107079.
[7] M.R. O'Masta, L. Dong, L. St-Pierre, H.N. Wadley, V.S. Deshpande, The fracture toughness of octet-truss lattices, J. Mech. Phys. Solids 98 (2017) 271–289.
[8] H. Gu, S. Li, M. Pavier, M.M. Attallah, C. Paraskevoulakos, A. Shterenlikht, Fracture of three-dimensional lattices manufactured by selective laser melting, Int. J. Solids Struct. 180–181 (2019) 147–159.
[9] Y. Liu, L. St-Pierre, N.A. Fleck, V.S. Deshpande, A. Srivastava, High fracture toughness micro-architectured materials, J. Mech. Phys. Solids 143 (2020) 104060.
[10] A.J.D. Shaikeea, H. Cui, M. O'Masta, X.R. Zheng, V.S. Deshpande, The toughness of mechanical metamaterials, Nat. Mater. 21 (2022) 297–304.
[11] J.B. Berger, H.N.G. Wadley, R.M. McMeeking, Mechanical metamaterials at the theoretical limit of isotropic elastic stiffness, Nature 543 (2017) 533–537.
[12] T. Tancogne-Dejean, M. Diamantopoulou, M.B. Gorji, C. Bonatti, D. Mohr, Metamaterials: 3D plate-lattices: an emerging class of low-density metamaterial exhibiting optimal isotropic stiffness, Adv. Mater. 30 (2018) 1870337.
[13] M.T. Hsieh, B. Endo, Y. Zhang, J. Bauer, L. Valdevit, The mechanical response of cellular materials with spinodal topologies, J. Mech. Phys. Solids 125 (2019) 401–419.
[14] M.F. Ashby, Mechanical properties of cellular solids, Metall. Trans. A 14 (1983) 1755–1769.
[15] L.J. Gibson, M.F. Ashby, Cellular Solids: Structure and Properties, 2nd ed., Cambridge University Press, 1997.
[16] J.Y. Chen, Y. Huang, M. Ortiz, Fracture analysis of cellular materials: a strain gradient model, J. Mech. Phys. Solids 46 (1998) 789–828.
[17] F. Lipperman, M. Ryvkin, M.B. Fuchs, Fracture toughness of two-dimensional cellular material with periodic microstructure, Int. J. Fract. 146 (2007) 279–290.
[18] K. Berkache, S. Phani, J.-F. Ganghoffer, Micropolar effects on the effective elastic properties and elastic fracture toughness of planar lattices, Eur. J. Mech. A, Solids 93 (2022) 104489.
[19] N.A. Fleck, X.M. Qiu, The damage tolerance of elastic-brittle, two-dimensional isotropic lattices, J. Mech. Phys. Solids 55 (2007) 562–588.
[20] I. Quintana-Alonso, N.A. Fleck, Damage tolerance of an elastic-brittle diamond-celled honeycomb, Scr. Mater. 56 (2007) 693–696.
[21] N.E. Romijn, N.A. Fleck, The fracture toughness of planar lattices: imperfection sensitivity, J. Mech. Phys. Solids 55 (2007) 2538–2564.
[22] I. Christodoulou, P.J. Tan, Crack initiation and fracture toughness of random Voronoi honeycombs, Eng. Fract. Mech. 104 (2013) 140–161.
[23] H. Gu, A. Shterenlikht, M. Pavier, Brittle fracture of three-dimensional lattice structure, Eng. Fract. Mech. 219 (2019) 106598.
[24] M.T. Hsieh, V.S. Deshpande, L. Valdevit, A versatile numerical approach for calculating the fracture toughness and R-curves of cellular materials, J. Mech. Phys. Solids 138 (2020) 103925.
[25] H.C. Tankasala, N.A. Fleck, The crack growth resistance of an elastoplastic lattice, Int. J. Solids Struct. 188–189 (2020) 233–243.
[26] J.S. Huang, L.J. Gibson, Fracture toughness of brittle honeycombs, Acta Metall. Mater. 39 (1991) 1617–1626.
[27] I. Quintana-Alonso, S.P. Mai, N.A. Fleck, D.C. Oakes, M.V. Twigg, The fracture toughness of a cordierite square lattice, Acta Mater. 58 (2010) 201–207.
[28] P.E. Seiler, H.C. Tankasala, N.A. Fleck, The role of defects in dictating the strength of brittle honeycombs made by rapid prototyping, Acta Mater. 171 (2019) 190–200.
[29] S. Luan, E. Chen, S. Gaitanaros, Energy-based fracture mechanics of brittle lattice materials, J. Mech. Phys. Solids 169 (2022) 105093.
[30] I. Quintana-Alonso, N.A. Fleck, Fracture of brittle lattice materials: a review, in: I.M. Daniel, E.E. Gdoutos, Y.D.S. Rajapakse (Eds.), Major Accomplishments in Composite Materials and Sandwich Structures, Springer Netherlands, Dordrecht, 2009, pp. 799–816.
[31] M. Omidi, L. St-Pierre, Fracture toughness of semi-regular lattices, Int. J. Solids Struct. (2023) 112233.
[32] H.C. Tankasala, V.S. Deshpande, N.A. Fleck, 2013 Koiter medal paper: Crack-tip fields and toughness of two-dimensional elastoplastic lattices, J. Appl. Mech. 82 (2015) 1–10.
[33] S.K. Maiti, M.F. Ashby, L.J. Gibson, Fracture toughness of brittle cellular solids, Scr. Mater. 18 (1984) 213–217.
[34] I. Schmidt, N.A. Fleck, Ductile fracture of two-dimensional cellular structures, Int. J. Fract. 111 (2001) 327–342.
[35] H. Gu, M. Pavier, A. Shterenlikht, Experimental study of modulus, strength and toughness of 2D triangular lattices, Int. J. Solids Struct. 152–153 (2018) 207–216.
[36] R. Williams, The Geometrical Foundation of Natural Structure: A Source Book of Design, Dover, New York, 1979.
[37] B. Grünbaum, G.C. Shephard, Tilings and Patterns, Dover, New York, 1987.
[38] A. Markou, L. St-Pierre, In-plane mechanical properties of demi-regular lattice materials, Preprint, https://doi.org/10.31224/2956, 2023.
[39] M.F. Ashby, H. Shercliff, D. Cebon, Materials: Engineering, Science, Processing and Design, Butterworth-Heinemann, 2018.
[40] S.D. Guest, J.W. Hutchinson, On the determinacy of repetitive structures, J. Mech. Phys. Solids 51 (2003) 383–391.
[41] R.G. Hutchinson, N.A. Fleck, The structural performance of the periodic truss, J. Mech. Phys. Solids 54 (2006) 756–782.
[42] X. Li, R.V. Kohn, Some results on the Guest–Hutchinson modes and periodic mechanisms of the Kagome lattice metamaterial, J. Mech. Phys. Solids 178 (2023) 105311.